hydrology

MDPI

Article

Assessment of Baseflow Separation Methods Used in the Estimations of Design-Related Storm Hydrographs Across Various Return Periods

Oscar E. Coronado-Hernández [1,*], Rafael D. Méndez-Anillo [2] and Manuel Saba [3]

[1] Instituto de Hidráulica y Saneamiento Ambiental, Universidad de Cartagena, Cartagena 130001, Colombia
[2] Escuela de Ingeniería, Arquitectura & Diseño, Universidad Tecnológica de Bolívar, Cartagena 131001, Colombia; rmendez@utb.edu.co
[3] Civil Engineering Program, Universidad de Cartagena, Cartagena 130001, Colombia; msaba@unicartagena.edu.co
* Correspondence: ocoronadoh@unicartagena.edu.co

Abstract: Accurately estimating storm hydrographs for various return periods is crucial for planning and designing hydrological infrastructure, such as dams and drainage systems. A key aspect of this estimation is the separation of baseflow from storm runoff. This study proposes a method for deriving storm hydrographs for different return periods based on hydrological station records. The proposed approach uses three baseflow separation methods: constant, linear, and master recession curve. A significant advantage of the proposed method over traditional rainfall–runoff approaches is its minimal parameter requirements during calibration. The methodology is tested on records from the Lengupá River watershed in Colombia, using data from the Páez hydrological station, which has a drainage area of 1090 km^2. The results indicate that the linear method yields the most accurate hydrograph estimates, as demonstrated by its lower root mean square error (RMSE) of 0.35%, compared to the other baseflow separation techniques, the values of which range from 2.92 to 3.02%. A frequency analysis of hydrological data was conducted using Pearson Type III and Generalized Extreme Value distributions to identify the most suitable statistical models for estimating extreme events regarding peak flow and maximum storm hydrograph volume. The findings demonstrate that the proposed methods effectively reproduce storm hydrographs for return periods ranging from 5 to 200 years, providing valuable insights for hydrological design, which can be employed using the data from stream gauging stations in rivers.

Keywords: baseflow separation; return period; stream gauging stations; storm hydrographs

Academic Editor: Yanfang Sang

Received: 21 May 2025
Revised: 13 June 2025
Accepted: 16 June 2025
Published: 19 June 2025

Citation: Coronado-Hernández, O.E.; Méndez-Anillo, R.D.; Saba, M. Assessment of Baseflow Separation Methods Used in the Estimations of Design-Related Storm Hydrographs Across Various Return Periods. *Hydrology* **2025**, *12*, 158. https://doi.org/10.3390/hydrology12060158

1. Introduction

The estimation of storm hydrographs associated with various return periods is fundamental for the design and development of engineering projects such as dams, diversion structures, urban drainage systems, and channels, among others [1–3]. To ensure the robustness of such designs, it is imperative to perform a rigorous calibration process, thereby generating reliable hydrographs that accurately represent the hydrological response of a catchment under varying storm conditions [4,5]. This estimation requires a comprehensive understanding of the hydrological cycle [6]. Upon reaching the Earth's surface, precipitation undergoes a series of processes before exiting the watershed. Initially, part of the precipitation is intercepted by vegetation and evaporates, while the remainder follows different pathways depending on the terrain and environmental conditions. These

pathways can be categorised into three types [6–8]: surface runoff, subsurface runoff, and groundwater runoff. A significant challenge arises in the estimation of groundwater runoff, as the analysis of aquifer systems is complex, and often, substantial costs are required when studying their interactions [9,10].

Groundwater runoff, the slowest form of runoff, originates from water that has infiltrated deeply into the soil and moved below the water level. Unlike surface runoff, which is directly associated with specific storm events, groundwater runoff progresses more gradually, often taking a long time to reach the watershed outlet [11]. This runoff is crucial in sustaining streamflow during dry periods and is responsible for baseflow in rivers and streams [12].

Storm hydrograph computation can be approached using methods based on rainfall–runoff relationships [13,14] or methods that rely solely on hydrological records [15,16]. While rainfall–runoff methods can physically describe all processes involved (precipitation, infiltration, surface runoff, subsurface runoff, and groundwater runoff), in practice, the calibration of these models is complex due to the multitude of parameters that must be estimated for each of the processes, particularly in large watersheds [17]. In the literature, these methods are commonly implemented using software packages such as HEC-HMS 4.12 [18], Mike SHE 2025 [19], SWAT +rev. 61 [20], EPA-SWMM 5.2.4 [21,22], and TETIS 9.1 [23], among others.

One alternative approach to storm hydrograph computation involves methods that rely only on records from hydrological stations [16]. The analysis of these methods requires the separation of storm runoff from baseflow volumes. The computation of storm hydrographs using these methods is generally more straightforward than rainfall–runoff models, as the calibration process is focused solely on baseflow separation methods. According to the literature, several techniques exist for baseflow separation, including constant, linear, master recession curve, Boussinesq approximation, and isotopic methods [6,24–26].

The primary objective of this research is to enhance the modelling of design-related storm hydrographs for various return periods by refining the parameters used in baseflow separation methods. Based on the following baseflow separation methods, new formulations for computing storm hydrographs for different return periods are proposed. The constant, linear, and master recession curve methods are simpler to implement than the Boussinesq approximation and isotopic methods, as the first set do not require field measurements.

To illustrate the practical application of the new formulations, this research applies the proposed methods to the Lengupá River watershed in Colombia, focusing on the Páez hydrological station, which has a drainage area of 1090 km^2. The results, derived using the baseflow methods implemented, indicate that the linear method provided the most accurate results, as evidenced by the lower root mean square error for hydrograph volume, compared to the constant and master recession curve methods.

The proposed method is a practical tool for estimating design-related storm hydrographs for various return periods more easily than traditional rainfall–runoff models. Unlike these models, the proposed approach effectively adjusts peak flow, baseflow rates, and maximum storm hydrograph volumes. This research provides hydrologists with a reliable and efficient tool for computing design-related hydrographs for various return periods.

2. Methodology

This study introduces the application of baseflow separation methods in the calculation of design-related hydrographs based on hydrological records corresponding to various return periods. Figure 1 outlines the methodology employed in this research, which comprises four main stages: (i) the analysis of three baseflow separation methods (constant, linear, and master recession curve); (ii) the calculation of the total hydrograph volume for

different return periods, considering the baseflow methods; (iii) the identification of the dataset to be used for a case study; and (iv) the generation of design-related hydrographs associated with the selected return periods.

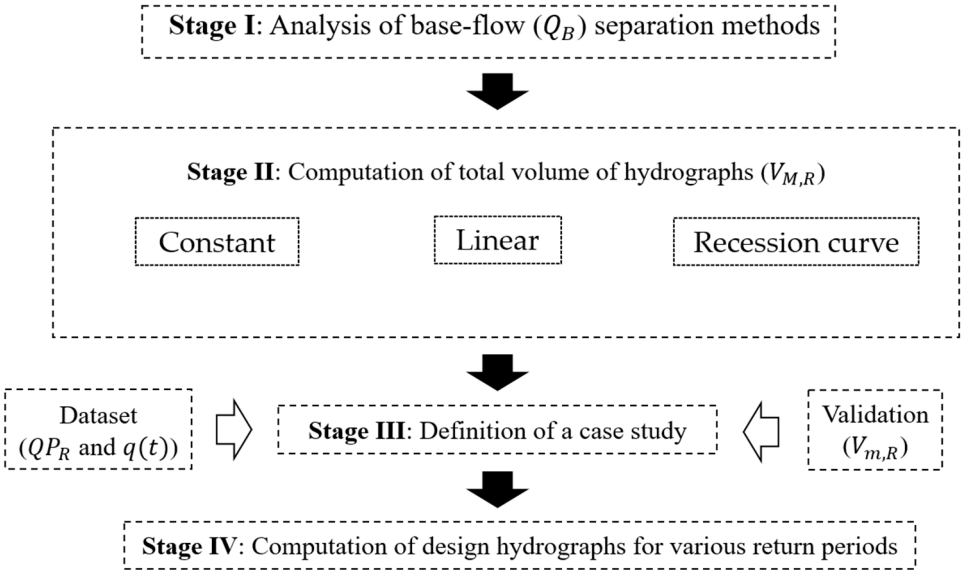

Figure 1. Methodology used in this research.

2.1. Computation of Design-Related Hydrographs

Understanding the base time of an isolated hydrograph is integral to hydrological modelling. Watershed characteristics influence the base time, and the area under the hydrograph represents the total runoff volume. Storm runoff originates from precipitation and typically forms a larger portion of the hydrograph, one which is distinguished from that of baseflow.

The equations for determining the total volume of a hydrograph corresponding to a given return period are derived from a mass balance between storm runoff and baseflow discharge (see Figure 2a). In this context, the total hydrograph volume is obtained as follows:

$$V_{M,R} = SR_R + BF_R \tag{1}$$

where $V_{M,R}$ is the total computed volume for a return period, SR_R is the storm runoff volume, and BF_R is the baseflow volume [16]. The subscript R refers to an analysed return period.

Figure 2a illustrates the variables employed to derive the formula for storm hydrographs. Figure 2b shows the characteristics of the dimensionless hydrograph $(U(t))$, as derived from recorded hydrographs, peak flows, and the baseflow estimation methods chosen for this study.

The baseflow volume for a given return period can be calculated as $BF_R = \int_0^T Q_{B,R}(t)dt$ based on the variables depicted in Figure 2a, where T represents the total duration of the hydrograph $(t_r - t_s)$. By considering the dimensionless hydrograph and the parameterisation shown in Figure 2b, the storm runoff volume can be determined as $SR_R = \int_0^T [QP_R - Q_{B,R}(t)]U(t)dt$. Then, the total volume may be calculated as follows:

$$V_{M,R} = \int_0^T Q_{B,R}(t)dt + QP_R \int_0^T U(t)dt - \int_0^T Q_{B,R}(t)U(t)dt \tag{2}$$

where Q_B is the baseflow function, QP is the peak flow, $U(t)$ is the dimentionless hydrograph, t is the time, and T is the total duration of a storm hydrograph.

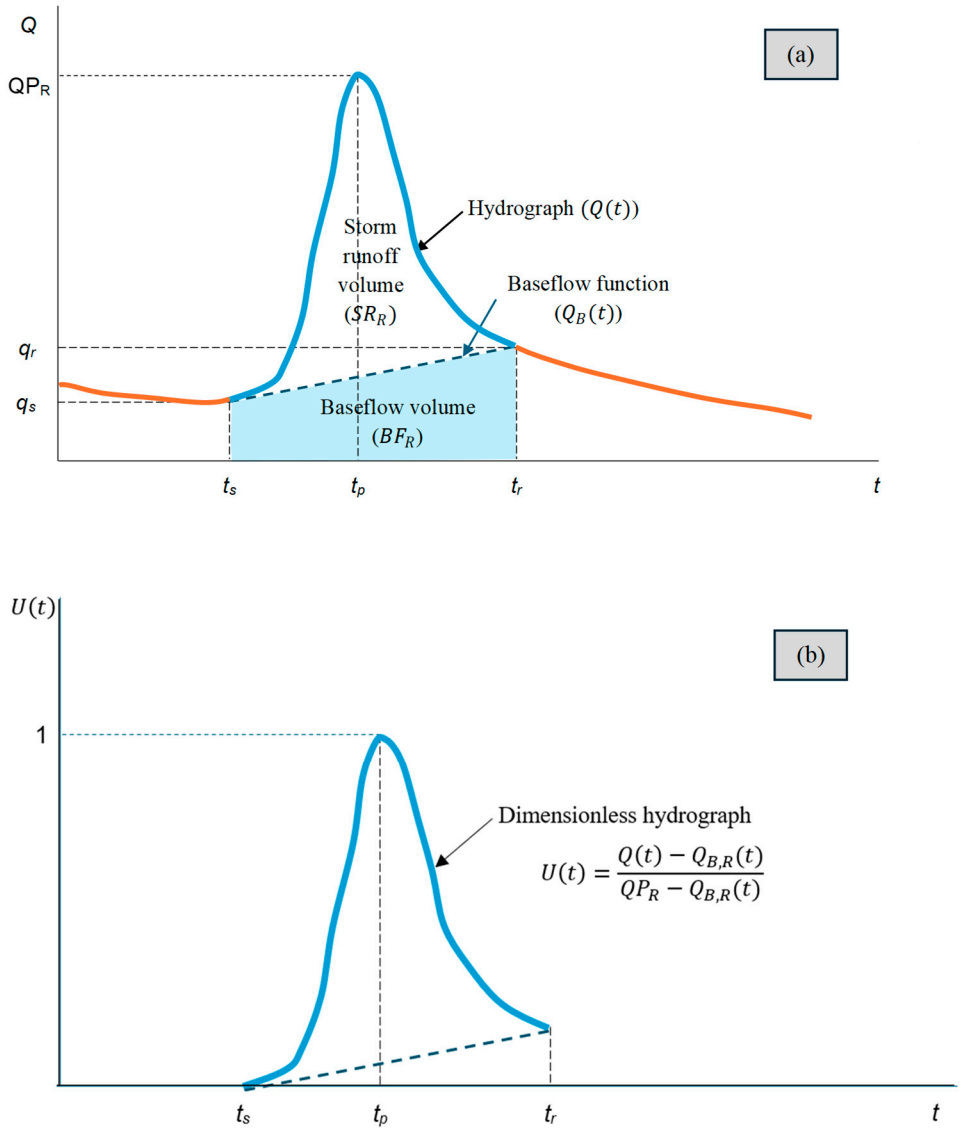

Figure 2. Hydrograph analysis: (**a**) components of a storm hydrograph; and (**b**) determination of the dimensionless hydrograph.

The calculation of design-related hydrographs is based on the following assumptions [16]: (i) the flood hydrograph for a given return period can be estimated using hydrological records alone, (ii) the total volume of a hydrograph can be determined as the sum of storm runoff and baseflow, (iii) the peak flow can be estimated using hydrological probability distributions, and (iv) the initial baseflow can be determined by considering the maximum value from the mean monthly series.

2.2. Baseflow Separation Methods and Hydrograph Volumes

Watercourses receive contributions from interacting aquifer systems, which must be appropriately characterised to estimate design-related hydrographs accurately. It is crucial to distinguish between the baseflow and storm runoff components in order to identify the portion associated with rainfall events and that generated by aquifer systems, respectively. This study applies three baseflow separation methods to calculate design-related hydrographs for various return periods, as shown in Figure 3. In this instance, baseflow formulas grounded in geometric principles are presented for practical application in real-world projects.

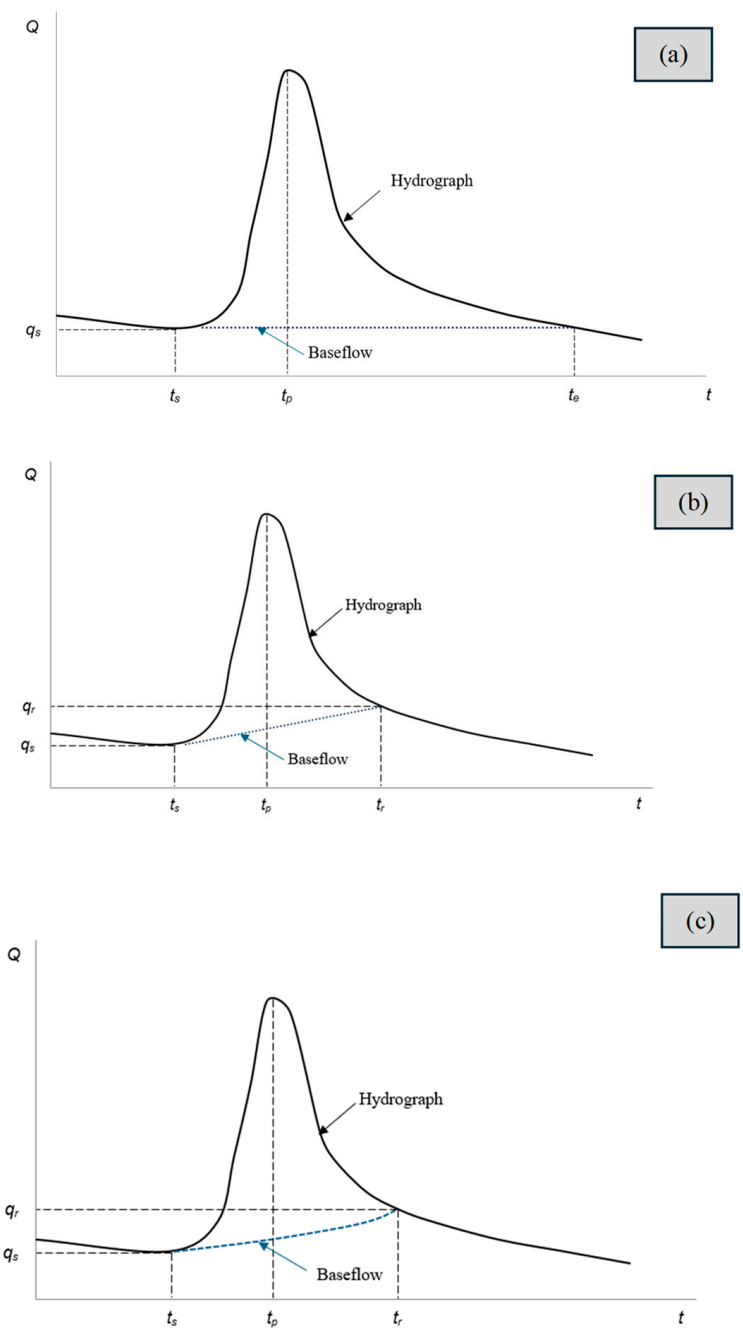

Figure 3. Baseflow separation methods: (**a**) constant, (**b**) linear, and (**c**) master recession curve.

2.2.1. Constant Baseflow

The constant baseflow method draws a straight line from the point at which storm runoff begins to its intersection with the recession limb of the hydrograph. Although this method can offer a reasonable approximation, particularly for minor storm events where groundwater levels remain unchanged, it typically overestimates the base time and the direct runoff volume. Mathematically, the baseflow function is given by Reference [6]:

$$Q_B(t) = \begin{cases} q & t < t_s \\ q_s & t_s \leq t \leq t_e \\ q & t_e < t \end{cases} \quad (3)$$

where q_s is the constant baseflow, q is the flow before and after the storm hydrograph, t_e is the final time of the hydrograph, and t_s is the start time of the hydrograph.

In this method, the baseflow remains constant throughout the flood event; hence, its corresponding equation is time independent. In this case, both q_s and QP are constant values. By substituting Equation (3) into Equation (2), the following expression is obtained:

$$V_{M,R} = q_s T + (QP_R - q_s) \int_0^T U(t)dt \tag{4}$$

2.2.2. Linear Separation

If the storm runoff process is conceptualised such that groundwater flow begins during the hydrograph recession, before the point assumed in the constant baseflow method, it is sufficient to identify the point on the recession limb where storm runoff ceases. Several approaches have been proposed to locate this point, the most common of which relies on identifying the inflexion point in the recession curve, the point at which the hydrograph transitions from concave to convex. Once the end of storm runoff has been determined, baseflow and storm runoff are separated by a straight line drawn from the point where storm runoff begins to the corresponding point on the recession limb [6].

Baseflow is a function of time (t_s) and discharge (q_s) at the lowest point of the discharge curve, as well as time t_r and discharge (q_r) at the inflexion point. Mathematically, the baseflow function is defined as:

$$Q_B(t) = \begin{cases} q & t < t_s \\ q_s + (t - t_s)\left[\frac{q_r - q_s}{t_r - t_s}\right] & t_s \leq t \leq t_r \\ q & t_r < t \end{cases} \tag{5}$$

where, q_r is the baseflow at the end of the storm hydrograph.

As the storm runoff volume must be calculated based on the baseflow during the storm event, the relevant portion satisfying this condition is extracted from Equation (5). Accordingly, the appropriate baseflow equation to be considered is as follows:

$$Q_B(t) = q_s + (t - t_s)\left[\frac{q_r - q_s}{t_r - t_s}\right] \tag{6}$$

The preceding equation represents a straight line, where the factor $(q_r - q_s)/(t_r - t_s)$ corresponds to the slope. For the sake of simplicity in presenting the equations, this factor is denoted by m, as follows:

$$Q_B(t) = q_s + m(t - t_s) \tag{7}$$

By plugging Equation (6) into Equation (2), then,

$$V_{M,R} = q_s T + \frac{mT^2}{2} - mt_s T + QP_R \int_0^T U(t)dt - \int_0^T [q_s + m(t - t_s)]U(t)dt \tag{8}$$

2.2.3. Master Recession Curve

The master recession curve method is employed to model groundwater storage flow. On this basis, it can be used to identify the point on the recession limb where storm runoff ceases and baseflow commences. This procedure involves the analysis of hydrographs from multiple storm events encompassing various volumes. The following functional form is commonly found to provide a reasonable fit to the data [27]:

$$Q_B(t) = q_s e^{-Kt} \tag{9}$$

where q_s is the discharge at time $t = 0$, and K is the exponential decay constant. The value of K can be determined using two points from the master recession curve.

In the master recession curve method, the baseflow function is exponential, and the value of K is derived from the hydrographs of the most extreme recorded storm events. In this equation, both q_s and K are treated as constants. By substituting Equation (9) into Equation (2), the following expression is obtained:

$$V_{M,R} = -\frac{q_s}{K}\left(e^{-KT} - 1\right) + QP_R\int_0^T U(t)dt - q_s\int_0^T e^{-Kt}U(t)dt \quad (10)$$

2.2.4. Other Baseflow Methods

The baseflow methods presented in Sections 2.2.1–2.2.3 can be applied using only the data from hydrological stations. This section introduces an analysis of baseflow separation methods based on the Boussinesq equation and isotopic techniques. However, applying these methods requires the determination of hydrogeological properties, which must be measured directly within aquifer systems. These methods can be employed by considering the following aspects:

- Boussinesq formula: This approach is derived from the governing equation for flow in saturated porous media. It provides a more physically based alternative to the empirical relationships described in Sections 2.2.1–2.2.3 and reduces the subjectivity typically associated with baseflow separation methods.
- Isotopic method: Certain water isotopes, such as oxygen-18 and deuterium, maintain stable isotopic compositions within specific components of the hydrological cycle, including aquifers and water bodies in which isotopic fractionation does not occur.

Appendix A provides the baseflow equations for the Boussinesq and isotopic methods and the derivation of the total hydrograph volume associated with various return periods [26,28,29].

2.3. Summary of Baseflow Separation and Hydrograph Volumes

A summary of the baseflow methods and the total storm hydrograph volumes associated with different return periods is provided in Table 1. This summary draws upon the analyses in Section 2.2 and the information in Appendix A.

Table 1. Summary of the baseflow equation and total volume.

Baseflow Method	Variable	Equation *
Constant	$Q_B(t)$	$Q_B(t) = \begin{cases} q & t < t_s \\ q_s & t_s \le t \le t_e \\ q & t_e < t \end{cases}$
	$V_{M,R}$	$V_{M,R} = q_s T + (QP_R - q_s)\sum_{t=0}^{T} U_t \Delta t$
Linear	$Q_B(t)$	$Q_B(t) = \begin{cases} q & t < t_s \\ q_s + (t - t_s)\left[\frac{q_r - q_s}{t_r - t_s}\right] & t_s \le t \le t_e \\ q & t_e < t \end{cases}$
	$V_{M,R}$	$V_{M,R} = q_s T + \frac{mT^2}{2} - mt_s T + QP_R\sum_{t=0}^{T} U_t \Delta t - \sum_{t=0}^{T}[q_s + m(t - t_s)]U_t \Delta t$
Master recession curve method	$Q_B(t)$	$Q_B(t) = q_0 e^{-Kt}$
	$V_{M,R}$	$V_{M,R} = \frac{q_s}{K}\left(1 - e^{-KT}\right) + QP_R\sum_{t=0}^{T} U_t \Delta t - q_s\sum_{t=0}^{T} e^{-Kt}U_t \Delta t$

Table 1. *Cont.*

Baseflow Method	Variable	Equation *
Boussinesq equation **	$Q_B(t)$	$Q_B(t) = \begin{cases} \left[{q_s}^{1-b} - (1-b)at\right]^{\frac{1}{1-b}} & \text{si } b \neq 1 \\ q_s e^{-at} & \text{si } b = 1 \end{cases}$
	$V_{M,R}$	$V_{M,R} = \begin{cases} \dfrac{\left[{q_s}^{1-b} - (1-b)aT\right]^{\frac{2-b}{1-b}} - {q_s}^{2-b}}{a(b-2)} + QP_R \sum_{t=0}^{T} U_t \Delta t - \sum_{t=0}^{T} \left[{q_s}^{1-b} - (1-b)at\right]^{\frac{1}{1-b}} U_t \Delta t & b \neq 1 \\ -\dfrac{q_s}{a} e^{-at} + QP_R \sum_{t=0}^{T} U_t \Delta t - q_s \sum_{t=0}^{T} e^{-at} U_t \Delta t & b = 1 \end{cases}$
Isotopic **	$Q_B(t)$	$Q_B(t) = \left(\frac{\delta_T - \delta_S}{\delta_B - \delta_S}\right) U(t)$
	$V_{M,R}$	$V_{M,R} = \left(\dfrac{\delta_T - \delta_S}{\delta_B - \delta_S} + QP_R\right) \sum_{t=0}^{T} U_t \Delta t - \left(\dfrac{\delta_T - \delta_S}{\delta_B - \delta_S}\right) \sum_{t=0}^{T} {U_t}^2 \Delta t$

Notes: * The equations are expressed using summation rather than integration, as the numerical resolution is intended to be performed accordingly. ** These methods have not been applied in the present study.

3. Practical Application

3.1. Case Study, Datasets, and Frequency Analysis

To examine the influence of baseflow separation methods on the determination of total hydrograph volumes associated with various return periods, a case study was conducted at the Lengupá River, Colombia. Table 2 presents the characteristics of the hydrological stations situated along the Lengupá River. All stations are located in the Boyacá department, within Colombia's Orinoquía region. IDEAM, the Spanish acronym for the Institute of Hydrology, Meteorology and Environmental Studies, operates these stations.

Table 2. Characteristics of the hydrological stations and available datasets.

Station Name	Station Code	Dataset Available	Latitude, Longitude
Páez	35087020	1976–2020	5.08, −73.07
San Agustín	35087010	1961–2021	4.86, −73.23
Casa de Máquinas	35087070	1982, 1999	4.90, −73.23
Chapasía	35087060	1999–2024	5.16, −73.09

The proposed model was implemented at the Páez station on the Lengupá River to demonstrate its applicability. Figure 4 shows the delineation of the watershed corresponding to this station. The watershed covers a drainage area of 1090 km^2, and the average longitudinal slope of the main channel is 0.064 m/m.

The annual peak flow series was derived from the records from the Páez station (Figure 5a). To compute the total hydrograph volume, storm hydrographs from 1996, 1997, and 1998 were selected, each lasting approximately one day. These hydrographs were chosen because they correspond to the dates on which the maximum peak flows were recorded.

In light of this, the maximum daily volume series was extracted as representative of the storm hydrograph (Figure 5b) [30]. Figure 5c presents the baseflow series, calculated by the authors, and using the mean monthly flow for the wettest month (July).

Based on the datasets presented in Figure 5, a frequency analysis was conducted using the Generalized Extreme Value, Gumbel, and Pearson Type III hydrological distributions. The distribution parameters were estimated using three fitting methods, namely, moments, maximum likelihood estimation, and L-moments, to identify the most suitable distribution. The Kolmogorov–Smirnov, Chi-Square, and Anderson–Darling statistical tests were employed to assess the goodness of fit. The HEC-SSP 2.3 software was used to perform the

calculations. Table 3 presents the results obtained; the best fit is highlighted in grey, while the second-best fit is indicated in blue.

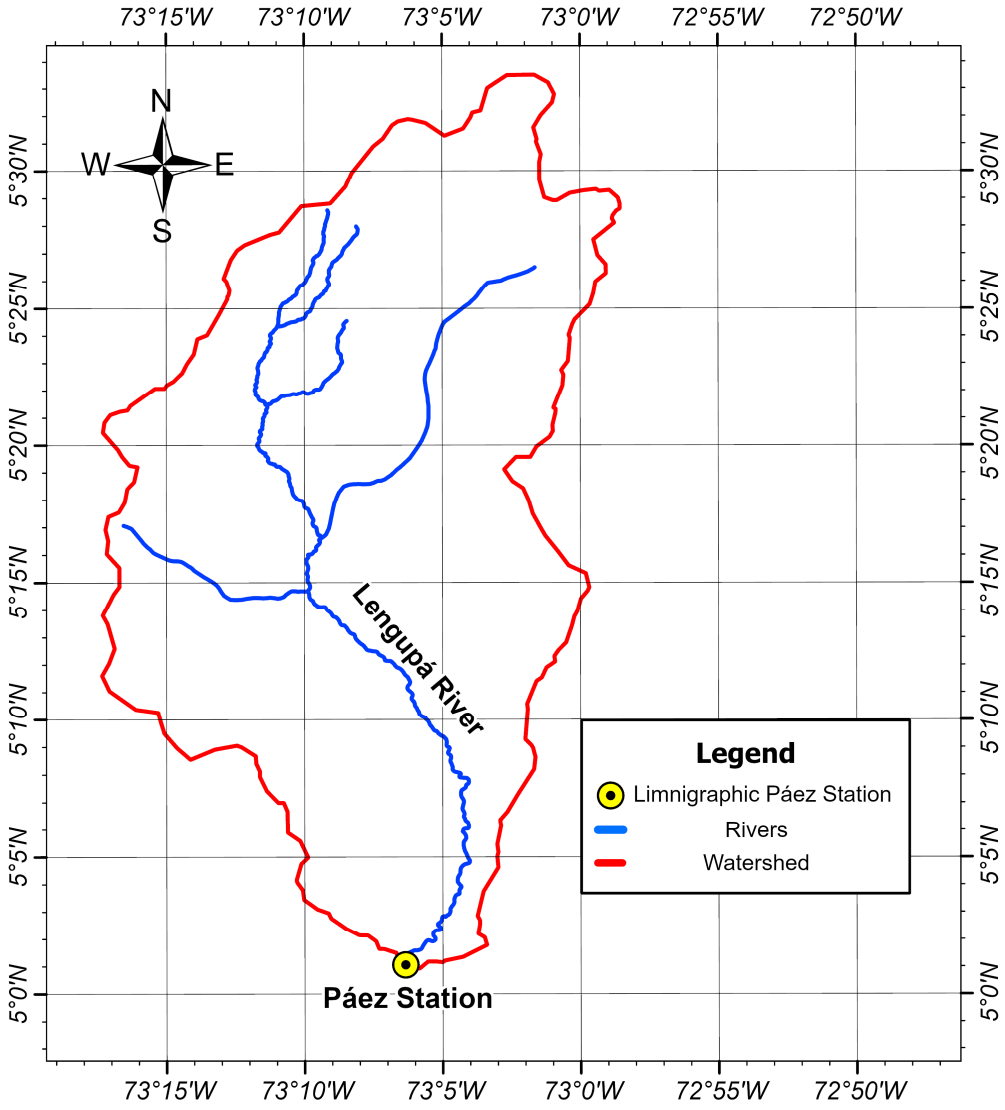

Figure 4. Delineation of the watershed for the Páez hydrological station located on the Lengupá River.

The frequency analysis was carried out using the Pearson Type III distribution for the peak flow series and the Generalized Extreme Value distribution for both the maximum daily volume and baseflow series [31]. In all cases, the distribution parameters were estimated using the L-moments method [32], as it provided the best fit, as shown in Table 3. Figure 6 presents the results obtained for the three analysed series.

The storm hydrographs from 1996, 1997, and 1998 were used to apply the methods proposed in this study. The dimensionless hydrograph was constructed based on the maximum peak flow and the corresponding peak time, as shown in Figure 7. The storm hydrographs show that peak times vary between 5 and 9 h.

3.2. Computation of Design-Related Hydrographs

Storm hydrographs for various return periods were calculated using the baseflow methods summarised in Table 1. Figure 8 illustrates the storm hydrographs generated using the model proposed in this research, which applies all three baseflow separation methods. The hydrographs were produced for return periods ranging from 5 to 200 years.

The proposed model effectively reproduces the peak flow, baseflow, and daily volume series associated with the different return periods for all baseflow separation methods.

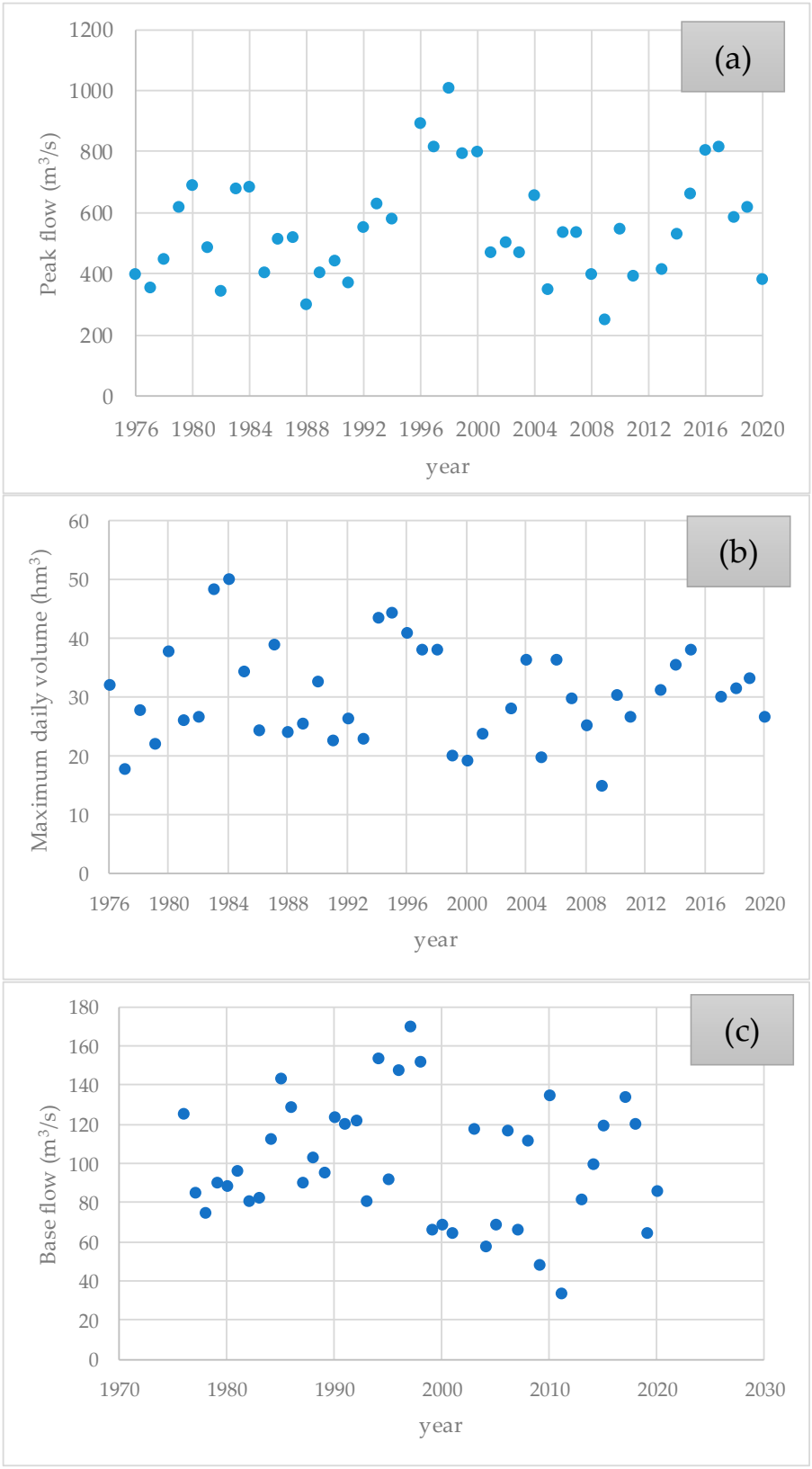

Figure 5. Annual values at the Páez hydrological station: (**a**) peak flow series, (**b**) maximum daily volume series, and (**c**) baseflow series.

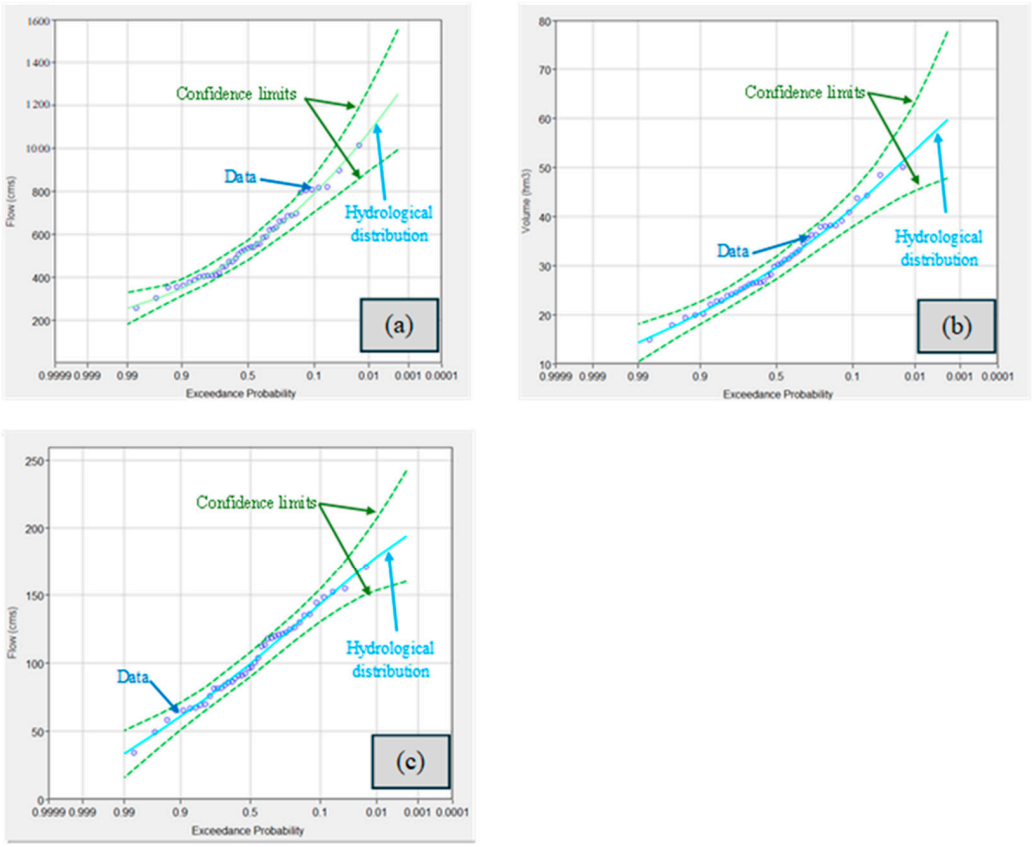

Figure 6. Frequency analysis results: (**a**) peak flow series, (**b**) maximum daily volume series, and (**c**) baseflow series.

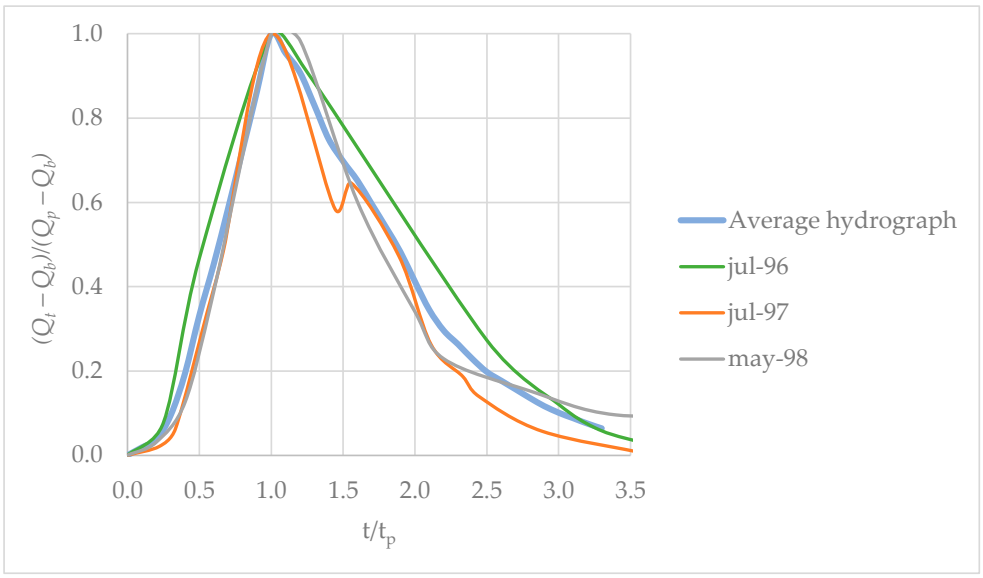

Figure 7. Computation of dimensionless hydrograph ($U(t)$) considering a linear baseflow separation method.

Table 3. Statistical tests for the annual series of the Páez station.

Distribution	Statistical Tests		
	Kolmogorov-Smirnov	**Chi-Square**	**Anderson-Darling**
Peak Flow series			
Pearson III (PM)	0.075	3.326	0.244
Generalized Extreme Value (PM)	0.077	3.326	0.240
Gumbel (PM)	0.085	1.837	0.265
Pearson III (LM)	0.066	2.953	0.189
Gumbel (LM)	0.070	2.581	0.202
Generalized Extreme Value (LM)	0.071	2.953	0.201
Pearson III (MLE)	0.071	2.953	0.197
Gumbel (MLE)	0.075	2.581	0.213
Generalized Extreme Value (MLE)	0.080	2.581	0.233
Daily volume series			
Generalized Extreme Value (PM)	0.080	3.333	0.147
Gumbel (PM)	0.082	4.476	0.319
Pearson III (PM)	0.083	3.333	0.162
Generalized Extreme Value (LM)	0.072	3.714	0.135
Pearson III (LM)	0.072	4.476	0.137
Gumbel (LM)	0.074	3.333	0.219
Gumbel (MLE)	0.063	4.857	0.181
Pearson III (MLE)	0.074	5.238	0.146
Generalized Extreme Value (MLE)	0.081	2.571	0.161
Baseflow series			
Generalized Extreme Value (PM)	0.085	4.857	0.236
Pearson III (PM)	0.088	3.333	0.272
Gumbel (PM)	0.132	10.571	0.666
Generalized Extreme Value (LM)	0.085	4.857	0.229
Pearson III (LM)	0.088	4.857	0.247
Gumbel (LM)	0.123	5.238	0.490
Generalized Extreme Value (MLE)	0.087	3.333	0.266
Pearson III (MLE)	0.094	3.333	0.276
Gumbel (MLE)	0.100	2.571	0.381

Notes: PM = standard product moment, MLE = maximum likelihood estimation, LM = L-moments. In addition, XXX = the best fit of the hydrological distribution, and XXX = the second-best fit of the hydrological distribution.

To generate the storm hydrograph, the following formulas were employed:

$$Q_{t,R} = U(t)(QP_R - Q_{B,R}) + Q_{B,R} \tag{11}$$

where Q_t is the storm hydrograph.

The parameters of the baseflow separation methods were computed. Parameters for the baseflow functions were estimated using the GRG nonlinear algorithm provided by the Solver of Microsoft Excel. The peak times obtained using all methods were of the same magnitude as those observed in the recorded storm hydrographs, varying from 4 to 9 h. The proposed model was calibrated solely using the parameters related to the baseflow separation methods. The peak time obtained for the constant and master recession curve methods was 9 h, higher than the 7 h observed for the linear method. The slope of the linear method was 9.32 $m^3/s/h$, while the recession constant (K) for the master recession curve was 0.016 h^{-1}.

To identify the most appropriate method for baseflow separation, the root mean square error (RMSE) was calculated as follows:

$$RMSE = \sqrt{\frac{1}{N}\sum_{i=1}^{N}\left(\frac{V_E - V_m}{V_E}\right)^2} \tag{12}$$

where V_E is the estimated hydrograph volume (see Figure 6b), V_m is the volume modelled using the proposed approach with the three baseflow separation methods, and N is the

total number of extreme events analysed. The estimated volume was determined through a frequency analysis of the series of maximum daily volumes (see Figure 6b).

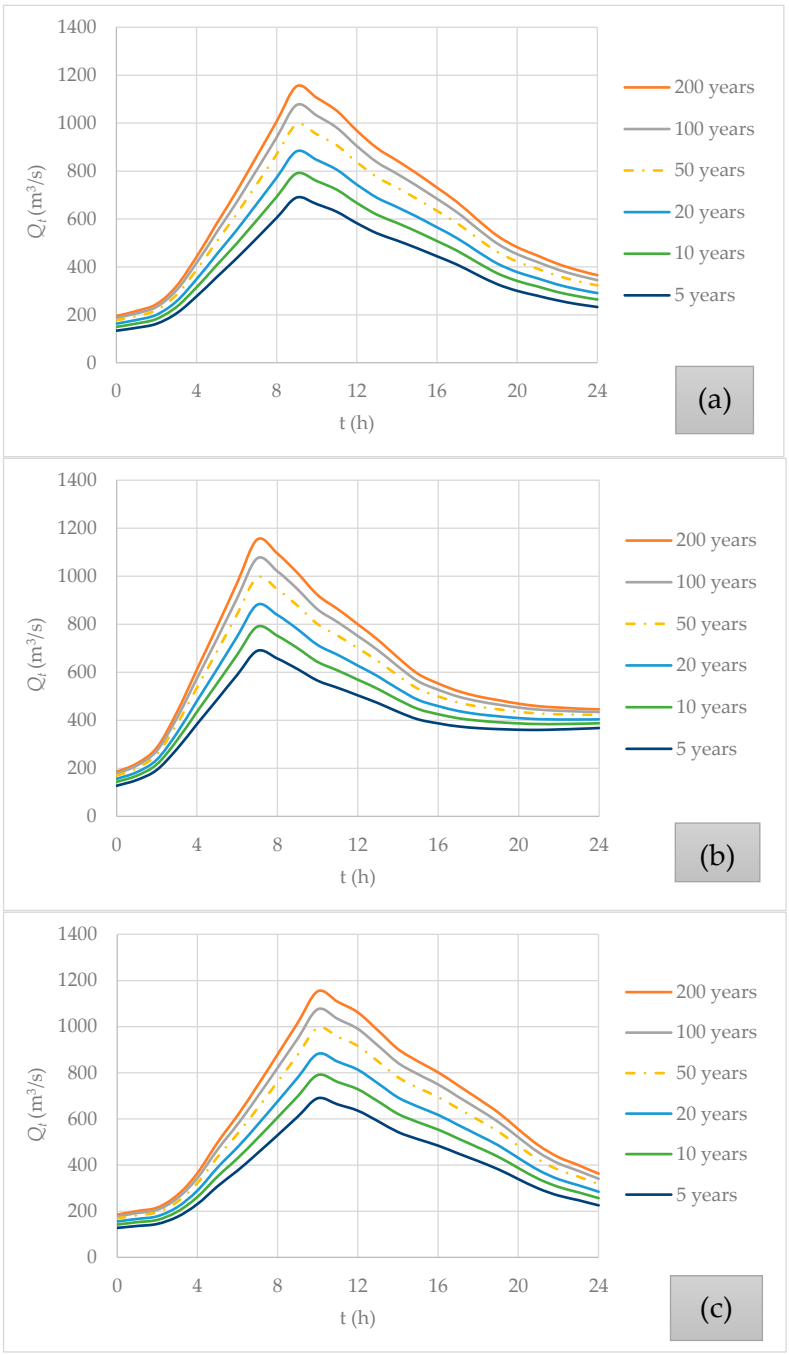

Figure 8. Computation of design-related storm hydrographs using the following baseflow separation methods: (**a**) constant, (**b**) linear, and (**c**) master recession curve.

Table 4 compares the modelled and estimated volumes and the corresponding RMSE for each baseflow separation method. The results indicate that the linear method provided the best fit, with an RMSE of 0.35%, while the constant and master recession curve methods yielded similar values. From a physical perspective, the linear method provided the best results, as the estimated storm hydrographs tend to exhibit this type of shape, as illustrated by the average dimensionless hydrograph shown in Figure 7.

Table 4. Comparison between observed and modelled storm hydrograph volumes for various return periods.

i	Return Period (Years)	Estimated Volume (hm^3) *	Computed Volume (hm^3) **		
			Constant	Linear	Master Recession Curve
1	200	56.4	57.7	56.5	58.2
2	100	53.5	54.0	53.4	54.4
3	50	50.4	50.2	50.2	50.5
4	20	45.8	44.7	45.6	45.0
5	10	41.8	40.3	41.7	40.5
6	5	37.3	35.3	37.5	35.4
$N = 6$		RMSE (%)	3.02	0.35	2.92

Notes: * Values obtained from Figure 6b. ** Values computed using the equations presented in Table 1.

4. Discussion

4.1. Advantages and Limitations

A key benefit of the proposed model is its versatility in tropical, semi-arid or mountainous regions, since it relies solely on hydrological data obtained from a gauging station. The proposed model may be used to size hydraulic structures in rivers equipped with gauging stations. Moreover, it can be applied to the analysis and design of diversion works, such as cofferdams, conduits, and multi-stage diversions, in riverine settings. It is also suitable for assessing extreme-event scenarios for projects adjacent to rivers. The main advantage of the proposed model, as combined with baseflow separation methods, is its low implementation cost compared to traditional rainfall–runoff approaches. The selection of baseflow methods is of the utmost importance in the determination of recorded hydrographs at stream gauge stations, a process which implies replicating existing conditions as closely as possible [6,25–27,33].

The proposed method's main limitation is that it cannot be applied to ungauged catchments or basins that lack reliable hydrological records. In regions with scarce datasets, rainfall–runoff models must be employed to calculate storm hydrographs associated with different return periods. Another disadvantage of the proposed model is that it cannot analyse sub-basins without installed stream gauging stations.

4.2. Regional Analysis and Dataset Comparison

4.2.1. Regional Analysis for the Case Study

To observe the behaviour of the maximum annual flows, records from the hydrological stations located along the Lengupá River in Colombia were analysed, considering all available stations listed by IDEAM. Table 2 presents a summary of the characteristics of these stations.

Only the hydrological stations of San Agustín and Chapasía, listed in Table 2, were used to fit the hydrological distributions; this decision was based on the lengths of the available annual peak flow records. Table 5 presents the results of the statistical goodness-of-fit tests: Kolmogorov–Smirnov, Chi-square, and Anderson–Darling, applied to the Pearson Type III, Generalized Extreme Value, and Gumbel distributions. The parameter estimation methods employed were moments, maximum likelihood estimation, and L-moments.

Table 5. Statistical tests of the peak flow annual series of stations located in the Lengupá River.

Distribution	Statistical Tests		
	Kolmogorov–Smirnov	**Chi-Square**	**Anderson–Darling**
Chapasía station			
Pearson III (PM)	0.093	NaN *	0.271
Generalized Extreme Value (PM)	0.105	NaN	0.295
Gumbel (PM)	0.126	0.909	0.487
Generalized Extreme Value (LM)	0.090	NaN	0.162
Pearson III (LM)	0.109	NaN	0.070
Gumbel (LM)	0.127	0.909	0.424
Generalized Extreme Value (MLE)	0.085	NaN	0.159
Gumbel (MLE)	0.109	0.909	0.344
Pearson III (MLE)	0.377	NaN	4.195
San Agustín station			
Generalized Extreme Value (PM)	0.125	16.526	0.73
Pearson III (PM)	0.127	15.368	0.77
Gumbel (PM)	0.139	15.754	1.027
Pearson III (LM)	0.119	13.439	0.695
Gumbel (LM)	0.121	10.737	0.812
Generalized Extreme Value (LM)	0.121	13.053	0.71
Gumbel (MLE)	0.115	11.509	0.723
Pearson III (MLE)	0.126	14.982	0.747
Generalized Extreme Value (MLE)	0.13	12.281	0.784

Notes: * NaN: Not applicable. In addition, XXX = the best fit of the hydrological distribution, and XXX = the second-best fit of the hydrological distribution.

The results are consistent with those obtained for the Páez station (see Table 3), as the Pearson Type III distribution using L-moments provided the best fit according to the Anderson–Darling test for the Chapasía station. The same distribution for the San Agustín station yielded the best results with the Anderson–Darling test and the second-best fit under the Kolmogorov–Smirnov test.

4.2.2. Comparison of an Additional Stream-Gauge Station

A comparison was made using data from an additional flow observation station. In this case, data from the Puente Balseadero station on the Magdalena River (station code 2104701; data obtained via IDEAM, Colombia) were analysed. This station covers a catchment area of 5584 km^2. The dataset utilized is available at Reference [33]. The results were extrapolated to the El Quimbo Hydropower Dam (Colombia) site, which has a drainage area of 6832 km^2. The linear baseflow method, applied for return periods ranging from 5 to 200 years, yielded a root mean square error (RMSE) of 1.98% (see Table 6). This value is higher than that obtained in the present case study (Lengupá station, as shown in Section 3), which achieved an RMSE of 0.35% for the same return periods. These findings are consistent, as larger drainage areas result in higher RMSE values. Implementing the linear and recession curve methods can improve accuracy, as they incorporate more parameters during the calibration phase.

4.3. Application of the Boussinesq Formula and Isotopic Methods

Applying these baseflow separation methods entails considerable costs for studies conducting hydrological analysis. In particular, the Boussinesq method requires measurements of groundwater levels, determination of soil properties along aquifer systems, and assessment of streambed conductance. The isotope method demands regular field

sampling and laboratory analysis, techniques which are not commonly undertaken by hydrologists worldwide.

Table 6. Comparison of the proposed model at the El Quimbo Hydropower Dam site, using the linear baseflow method.

i	Return Period (Years)	Estimated Volume (hm^3)	Computed Volume (hm^3)
1	200	322.02	319.0
2	100	298.69	295.4
3	50	276.23	271.7
4	20	240.91	240.1
5	10	222.05	215.7
6	5	196.69	190.3
$N = 6$	RMSE (%)	1.98%	

5. Conclusions

In this study, a hydrological method based on data from stream gauging stations has been developed, incorporating five baseflow separation techniques: the constant baseflow method, the straight-line method, the master recession curve method, a physically based method derived from the analytical solution of the Boussinesq equation, and a chemically based isotopic method.

The proposed model's primary advantage over traditional rainfall–runoff approaches is that it relies solely on hydrological records from a stream gauging station. Moreover, the only parameters requiring calibration pertain to the baseflow separation methods used in the calculations. This model's application necessitates information on peak flows, initial baseflows, and the maximum volume values of storm hydrographs associated with different return periods.

Accurate separation of baseflow from storm runoff is paramount in improving the estimation of design-related storm hydrographs. The methodology implemented in this research enables the computation of design-related storm hydrographs for various return periods, using hydrological records from stream gauging stations.

The proposed method was applied to a case study at the Páez stream gauging station, located on the Lengupá River in Colombia, which has a drainage area of 1090 km^2. The results of the model's application led to the following conclusions:

- The frequency analysis demonstrated that the L-moments technique was the most effective approach in calculating peak flows, initial baseflows, and the maximum volume values of storm hydrographs for different return periods.
- The findings confirm that the statistical models used are well-suited for predicting events with return periods ranging from 5 to 200 years, as the proposed model successfully reproduces extreme values of peak flows, initial baseflows, and storm hydrograph volumes.
- The linear baseflow separation method provided the highest accuracy, with a root mean square error (RMSE) of 0.35% in terms of maximum volume across different return periods. However, the constant and master recession curve methods also yielded reliable results, with RMSE values of 3.02% and 2.92%, respectively. These results indicate that the proposed model is a valuable tool for hydrologists in computing storm hydrographs for different return periods.

Future research should focus on further applying the demonstrated formulas, particularly those based on the Boussinesq equation (physically based) and the isotopic method (chemically based), to enhance the robustness of the proposed methodology.

Author Contributions: Conceptualization, R.D.M.-A. and O.E.C.-H.; methodology, R.D.M.-A., O.E.C.-H., and M.S.; formal analysis, R.D.M.-A. and O.E.C.-H.; writing—original draft preparation, R.D.M.-A. and O.E.C.-H.; writing—review and editing, M.S. All authors have read and agreed to the published version of the manuscript.

Funding: This research received no external funding.

Data Availability Statement: The databases used are available in this article.

Conflicts of Interest: The authors declare no conflicts of interest.

Nomenclature

The following abbreviations are employed in this article:

A	Watershed area (km^2)
a, b	Parameters of the Boussinesq equation
B	Aquifer width (m)
C_{sample}	Concentration sample
C_{SMOW}	Concentration of isotopes
BF	Baseflow volume (m^3)
D	Depth of an aquifer (m)
d	Discharge of an aquifer (m^3/s)
h	Groundwater level (m)
K	Decay exponent (s^{-1})
k	Saturated hydraulic conductivity of the unconfined aquifer (m/s)
L	Total length of contributing channels (m)
m	Slope or factor of the linear baseflow method ($m^3/s/h$)
N	Number of analysed storm hydrographs (-)
Q_B	Baseflow discharge (m^3/s)
Q_t	Total discharge of a storm hydrograph (m^3/s)
QP	Peak flow (m^3/s)
q	Flow before and after a storm hydrograph (m^3/s)
q_s	Constant baseflow or initial baseflow discharge (m^3/s)
q_r	Final discharge of the baseflow function (m^3/s)
R_d	Drainage density (1/m)
$RMSE$	Root mean square error (%)
SR	Storm runoff volume (m^3)
$U(t)$	Dimensionless hydrograph (-)
u	Auxiliar variable for integration purposes
T	Duration of a storm hydrograph (s)
t	Time (s)
t_p	Peak time (s)
t_s	Initial time of a recorded hydrograph (s)
t_e/t_r	Final time of a recorded hydrograph (s), where e corresponds to a constant baseflow and r corresponds to linear and recession curve methods
V_M	Total modelled volume (m^3)
V_m	Total measured volume (m^3)
x	Horizontal distance (m)
δ	Isotopic content (‰)
Subscripts	
R	Refers to a return period (years)

Appendix A. Demonstration of Additional Baseflow Methods

Appendix A.1. Based on the Boussinesq Equation

When the effect of capillarity above the groundwater table is neglected and the Dupuit–Forchheimer approximation is applied, the one-dimensional Boussinesq equation describes the transient elevation of the groundwater level $h(x,t)$ above a horizontal impermeable layer:

$$\frac{\partial h}{\partial t} = \frac{k}{\varphi}\frac{\partial}{\partial x}\left(h\frac{\partial h}{\partial x}\right) \tag{A1}$$

where k is the saturated hydraulic conductivity of the unconfined aquifer, φ is the drainable porosity, t is time, and x is the horizontal distance [25].

For a fully penetrating stream ($h(0,t) = 0$) draining from an initially saturated aquifer ($h(x,0) = D$), where D is the depth of the aquifer of finite width B, the resulting discharge $d(t)$ for short times is given by Reference [28]:

$$d(t) = 0.332(k\varphi)^{1/2}D^{3/2}t^{-1/2} \tag{A2}$$

When the recession extends across the entire width of the aquifer, the discharge for long times becomes

$$d(t') = \frac{0.862kD^2}{B\left[1 + 1.115\left(\frac{kD}{\varphi B^2}\right)t'\right]^2} \tag{A3}$$

The exact time at which groundwater discharge begins in Equation (A2) is generally unknown. Therefore, Reference [28] proposed that the slope of the hydrograph recession (dQ/dt) could be analysed as a function of discharge (Q). For Equations (A2) and (A3), the recession slope can be expressed as

$$\frac{dQ(t)}{dt} = -aQ^b(t) \tag{A4}$$

where $Q = 2Lqdl$ (where L is the total length of the contributing channels) is the measured discharge, and a and b are constant values. With appropriate expressions for the drainage density $R_d = LA^{-1}$, where A is the catchment area and an effective width $B = 2R_d^{-1}$ for natural catchments, the constants in Equation (A4) are as follows:

$$a_1 = \frac{1.133}{k\varphi D^3L^2}; \quad b_1 = 3 \tag{A5}$$

For a short-term solution, the following analysis is conducted:

$$a_2 = \frac{4.804k^{1/2}L}{\varphi A^{3/2}}; \quad b_2 = \frac{3}{2} \tag{A6}$$

Or, for a long-term solution, Equation (A4) has two straight lines, with slopes of 3 and 1.5, intercepting at a_1 and a_2, and corresponding to Equations (A5) and (A6), respectively. The general solution to Equation (A4) is

$$Q_B(t) = \begin{cases} \left[{q_s}^{1-b} - (1-b)at\right]^{\frac{1}{1-b}} & \text{si } b \neq 1 \\ q_s e^{-at} & \text{si } b = 1 \end{cases} \tag{A7}$$

In the method based on the analytical solutions of the Boussinesq equation, the baseflow function corresponds to a binomial raised to a power, the value of which essentially

depends on the soil parameters. Initially, the solution is obtained for the case in which $b \neq 1$ by substituting Equation (A7) into Equation (2), as follows:

$$V_{M,R} = \int_0^T \left[{q_s}^{1-b} - (1-b)at\right]^{\frac{1}{1-b}} dt + QP_R \int_0^T U(t)dt - \int_0^T \left[{q_s}^{1-b} - (1-b)at\right]^{\frac{1}{1-b}} U(t)dt \quad \text{(A8)}$$

To solve the integral, the following substitution is applied:

$$u = {q_s}^{1-b} - (1-b)at; \quad dt = -\frac{du}{(1-b)a} \quad \text{(A9)}$$

Then,

$$\begin{aligned} \int \left[{q_s}^{1-b} - (1-b)at\right]^{\frac{1}{1-b}} dt &= -\tfrac{1}{(1-b)a} \int u^{\frac{1}{1-b}} du = -\tfrac{1}{(1-b)a} \tfrac{u^{\frac{1}{1-b}+1}}{\frac{1}{1-b}+1} \\ &= -\tfrac{1}{(1-b)a} \tfrac{u^{\frac{2-b}{1-b}}}{\frac{2-b}{1-b}} = \tfrac{\left[{q_0}^{1-b} - (1-b)at\right]^{\frac{2-b}{1-b}}}{a(b-2)} \end{aligned} \quad \text{(A10)}$$

By evaluating the resulting expression over the interval from $t = 0$ to $t = T$, the following is obtained:

$$\int_0^T \left[{q_s}^{1-b} - (1-b)at\right]^{\frac{1}{1-b}} dt = \frac{\left[{q_s}^{1-b} - (1-b)aT\right]^{\frac{2-b}{1-b}} - {q_s}^{2-b}}{a(b-2)} \quad \text{(A11)}$$

The equation for computing a storm hydrograph for the case where $b \neq 1$ is

$$\begin{aligned} V_{M,R} = &\tfrac{\left[{q_s}^{1-b} - (1-b)aT\right]^{\frac{2-b}{1-b}} - {q_0}^{2-b}}{a(b-2)} + QP_R \textstyle\int_0^T U(t)dt \\ &- \textstyle\int_0^T \left[{q_s}^{1-b} - (1-b)at\right]^{\frac{1}{1-b}} U(t)dt \end{aligned} \quad \text{(A12)}$$

To obtain the solution for the case where $b = 1$, the corresponding part of Equation (A7) is substituted into Equation (2), as follows:

$$V_{M,R} = \int_0^T q_s e^{-at} dt + QP_R \int_0^T U(t)dt - \int_0^T q_s e^{-at} U(t)dt \quad \text{(A13)}$$

By solving the corresponding integral, the equation becomes

$$V_{M,R} = -\frac{q_s}{a} e^{-at} + QP_R \int_0^T U(t)dt - q_s \int_0^T e^{-at} U(t)dt \quad \text{(A14)}$$

Appendix A.2. Isotopic Method

Certain water isotopes, such as oxygen-18 and deuterium, possess isotopic signatures that are preserved in specific systems of the hydrological cycle, including aquifers and certain bodies of water, where fractionation does not occur. The concentrations of oxygen-18 and deuterium in water are expressed as the difference in per mil of the D/H and ${}^{18}O/{}^{16}O$ ratios relative to the same ratios in ocean water (SMOW, Standard Mean Ocean Water), referred to as the reference sample. This difference is expressed as a content value, the notation of which is δ [26]:

$$\delta = \frac{C_{sample} - C_{SMOW}}{C_{SMOW}} \quad \text{(A15)}$$

where δ is the isotopic content, C_{sample} is the concentration of Escribaa quí la ecuación. ${}^{18}O/{}^{16}O$ for oxygen and D/H for deuterium in the sample, and C_{SMOW} is the concentration of isotopes (SMOW) in the reference sample. During the various stages of the hydrological

cycle, water isotopes acquire isotopic content due to phase changes, specifically, evaporation and condensation. Evaporated waters have higher isotopic contents, while rainwaters have lower isotopic contents.

The mass conservation equation, taking as the control volume a segment of a river in which the inflows and outflows are constant and assuming that there are no losses in that section, allows for the relation of each component of the flow to its corresponding isotopic content, as follows:

$$Q_T\delta_T = Q_B\delta_B + Q_S\delta_S \tag{A16}$$

where Q_T, Q_B, and Q_S represent the total flow in the river, baseflow, and surface runoff, respectively, and δ_T, δ_B, and δ_S correspond to the isotopic contents of the total flow in the river, baseflow, and surface runoff, respectively. By applying the principle of mass conservation, then,

$$Q_B = \left(\frac{\delta_T - \delta_S}{\delta_B - \delta_S}\right)U(t) \tag{A17}$$

The isotopic contents required in Equation (A17) necessitate isotopic content data that are the weighted averages of the different flows they represent. The sampling is designed to obtain meaningful and representative averages of the isotopic content at each component's temporal and spatial scales. Equation (A17) is used to separate the baseflow into two components. This equation represents the proportion of the baseflow relative to the total flow passing through the river, based on the isotopic contents of surface runoff, baseflow, and total flow. Estimating the previous values involves measuring variables such as precipitation and discharge at appropriate temporal and spatial scales [29].

The baseflow function for this method is a function of time, as defined by the total flow function. By substituting Equation (A17) into Equation (2), the following is obtained:

$$V_{M,R} = \left(\frac{\delta_T - \delta_S}{\delta_B - \delta_S} + QP_R\right)\int_0^T U(t)dt - \left(\frac{\delta_T - \delta_S}{\delta_B - \delta_S}\right)\int_0^T [U(t)]^2 dt \tag{A18}$$

References

1. Basso, S.; Merz, R.; Tarasova, L.; Miniussi, A. Extreme Flooding Controlled by Stream Network Organization and Flow Regime. *Nat. Geosci.* **2023**, *16*, 339–343. [CrossRef]
2. Chikamori, H. Rainfall-Runoff Analysis of Flooding Caused by Typhoon RUSA in 2002 in the Gangneung Namdae River Basin, Korea. *J. Nat. Disaster Sci.* **2004**, *26*, 95–100.
3. Crookston, B.M.; Erpicum, S. Hydraulic Engineering of Dams. *J. Hydraul. Res.* **2022**, *60*, 184–186. [CrossRef]
4. Assaf, M.N.; Manenti, S.; Creaco, E.; Giudicianni, C.; Tamellini, L.; Todeschini, S. New Optimization Strategies for SWMM Modeling of Stormwater Quality Applications in Urban Area. *J. Environ. Manag.* **2024**, *361*, 121244. [CrossRef]
5. Dotto, C.B.S.; Kleidorfer, M.; Deletic, A.; Fletcher, T.D.; McCarthy, D.T.; Rauch, W. Stormwater Quality Models: Performance and Sensitivity Analysis. *Water Sci. Technol.* **2010**, *62*, 837–843. [CrossRef]
6. Chow, V.T.; Maidment, D.R.; Mays, L.W. *Applied Hydrology*; McGraw-Hill International Editions: New York, NY, USA, 1988; ISBN 0-07-010810-2.
7. Ross, C.A.; Ali, G.; Bansah, S.; Laing, J.R. Evaluating the Relative Importance of Shallow Subsurface Flow in a Prairie Landscape. *Vadose Zone J.* **2017**, *16*, 1–20. [CrossRef]
8. Bronstert, A.; Niehoff, D.; Schiffler, G.R. Modelling Infiltration and Infiltration Excess: The Importance of Fast and Local Processes. *Hydrol. Process.* **2023**, *37*, e14875. [CrossRef]
9. Barthel, R.; Banzhaf, S. Groundwater and Surface Water Interaction at the Regional-Scale—A Review with Focus on Regional Integrated Models. *Water Resour. Manag.* **2016**, *30*, 1–32. [CrossRef]
10. Nogueira, G.E.H.; Partington, D.; Heidbüchel, I.; Fleckenstein, J.H. Combined Effects of Geological Heterogeneity and Discharge Events on Groundwater and Surface Water Mixing. *J. Hydrol.* **2024**, *638*, 131467. [CrossRef]
11. Aranguren-Díaz, Y.; Galán-Freyle, N.J.; Guerra, A.; Manares-Romero, A.; Pacheco-Londoño, L.C.; Romero-Coronado, A.; Vidal-Figueroa, N.; Machado-Sierra, E. Aquifers and Groundwater: Challenges and Opportunities in Water Resource Management in Colombia. *Water* **2024**, *16*, 685. [CrossRef]

12. Briggs, M.A.; Newman, C.; Benton, J.R.; Rey, D.M.; Konrad, C.P.; Ouellet, V.; Torgersen, C.E.; Gruhn, L.; Fleming, B.J.; Gazoorian, C.; et al. James Buttle Review: The Characteristics of Baseflow Resilience Across Diverse Ecohydrological Terrains. *Hydrol. Process.* **2025**, *39*, e70101. [CrossRef]
13. Baig, F.; Sherif, M.; Faiz, M.A. Quantification of Precipitation and Evapotranspiration Uncertainty in Rainfall-Runoff Modeling. *Hydrology* **2022**, *9*, 51. [CrossRef]
14. Jehanzaib, M.; Ajmal, M.; Achite, M.; Kim, T.-W. Comprehensive Review: Advancements in Rainfall-Runoff Modelling for Flood Mitigation. *Climate* **2022**, *10*, 147. [CrossRef]
15. Rivera Trejo, F.; Escalante Sandoval, C. Análisis Comparativo de Técnicas de Estimación de Avenidas de Diseño. *Ing. Del Agua* **1999**, *6*, 49–54. [CrossRef]
16. Coronado-Hernández, O.E.; Fuertes-Miquel, V.S.; Arrieta-Pastrana, A. The Development of a Hydrological Method for Computing Extreme Hydrographs in Engineering Dam Projects. *Hydrology* **2024**, *11*, 194. [CrossRef]
17. Shin, M.-J.; Kim, C.-S. Analysis of the Effect of Uncertainty in Rainfall-Runoff Models on Simulation Results Using a Simple Uncertainty-Screening Method. *Water* **2019**, *11*, 1361. [CrossRef]
18. Dotson, H.W. Watershed Modeling with HEC-HMS (Hydrologic Engineering Centers-Hydrologic Modeling System) Using Spatially Distributed Rainfall. In *Coping with Flash Floods*; Springer: Berlin/Heidelberg, Germany, 2001; pp. 219–230.
19. Ma, L.; He, C.; Bian, H.; Sheng, L. MIKE SHE Modeling of Ecohydrological Processes: Merits, Applications, and Challenges. *Ecol. Eng.* **2016**, *96*, 137–149. [CrossRef]
20. Swain, S.; Mishra, S.K.; Pandey, A.; Pandey, A.C.; Jain, A.; Chauhan, S.K.; Badoni, A.K. Hydrological Modelling through SWAT over a Himalayan Catchment Using High-Resolution Geospatial Inputs. *Environ. Chall.* **2022**, *8*, 100579. [CrossRef]
21. Hodges, B.R.; Sharior, S.; Tiernan, E.D.; Jenkins, E.; Riaño-Briceño, G.; Davila-Hernandez, C.; Madadi-Kandjani, E.; Yu, C.-W. Introducing SWMM5+. *J. Environ. Eng.* **2024**, *150*, 02524003. [CrossRef]
22. Campisano, A.; Catania, F.V.; Modica, C. Evaluating the SWMM LID Editor Rain Barrel Option for the Estimation of Retention Potential of Rainwater Harvesting Systems. *Urban Water J.* **2017**, *14*, 876–881. [CrossRef]
23. Quintero, F.; Velásquez, N. Implementation of TETIS Hydrologic Model into the Hillslope Link Model Framework. *Water* **2022**, *14*, 2610. [CrossRef]
24. Duncan, H.P. Baseflow Separation—A Practical Approach. *J. Hydrol.* **2019**, *575*, 308–313. [CrossRef]
25. Szilagyi, J.; Parlange, M.B. Baseflow Separation Based on Analytical Solutions of the Boussinesq Equation. *J. Hydrol.* **1998**, *204*, 251–260. [CrossRef]
26. International Atomic Energy Environmental Isotopes in the Hydrological Cycle: Principles and Applications, v. II: Atmospheric Water. 2001. Available online: https://unesdoc.unesco.org/ark:/48223/pf0000149442 (accessed on 15 May 2025).
27. Yang, H.; Choi, H.T.; Lim, H. Applicability Assessment of Estimation Methods for Baseflow Recession Constants in Small Forest Catchments. *Water* **2018**, *10*, 1074. [CrossRef]
28. Brutsaert, W.; Nieber, J.L. Regionalized Drought Flow Hydrographs from a Mature Glaciated Plateau. *Water Resour. Res.* **1977**, *13*, 637–643. [CrossRef]
29. Gómez, S.; Guzmán, J. Separation of Base Flow in Upper Part of the Lebrija River Basin. *Rev. Fac. Ing. Univ. Antioq.* **2011**, *61*, 41–52. [CrossRef]
30. Villalba-Barrios, A.F.; Coronado-Hernández, O.E.; Fuertes-Miquel, V.S.; Coronado-Hernández, J.R.; Ramos, H.M. Statistical Approach for Computing Base Flow Rates in Gaged Rivers and Hydropower Effect Analysis. *Hydrology* **2023**, *10*, 137. [CrossRef]
31. Chen, X.; Shao, Q.; Xu, C.Y.; Zhang, J.; Zhang, L.; Ye, C. Comparative Study on the Selection Criteria for Fitting Flood Frequency Distribution Models with Emphasis on Upper-Tail Behavior. *Water* **2017**, *9*, 320. [CrossRef]
32. Anghel, C.G. Revisiting the Use of the Gumbel Distribution: A Comprehensive Statistical Analysis Regarding Modeling Extremes and Rare Events. *Mathematics* **2024**, *12*, 2466. [CrossRef]
33. Coronado-Hernández, O.E. Consideraciones de Incertidumbre en la Estimación de Hidrogramas de Diseño de Estructuras de Desviación y Rebosaderos en Presas. Master's Dissertation, Universidad de los Andes, Bogotá, Colombia, 2010.